Observational Study

Medicine®

OPEN

Discriminative analysis of schizophrenia using support vector machine and recursive feature elimination on structural MRI images

Xiaobing Lu, MD[a,c], Yongzhe Yang, BE[b,d,f], Fengchun Wu, MD[a,c], Minjian Gao, BE[g], Yong Xu, DE[g], Yue Zhang, BE[b], Yongcheng Yao, BE[b], Xin Du, BE[b], Chengwei Li, BE[b], Lei Wu, BE[b,d,f], Xiaomei Zhong, MD[a,c], Yanling Zhou, MD[a], Ni Fan, MD[a], Yingjun Zheng, MD[a], Dongsheng Xiong, DE[b], Hongjun Peng, MD[e], Javier Escudero, DE[l], Biao Huang, MD[d,f], Xiaobo Li, DE[h,i,j], Yuping Ning, MD[a,c,*], Kai Wu, MD[a,b,c,k,*]

Abstract

Structural abnormalities in schizophrenia (SZ) patients have been well documented with structural magnetic resonance imaging (MRI) data using voxel-based morphometry (VBM) and region of interest (ROI) analyses. However, these analyses can only detect group-wise differences and thus, have a poor predictive value for individuals. In the present study, we applied a machine learning method that combined support vector machine (SVM) with recursive feature elimination (RFE) to discriminate SZ patients from normal controls (NCs) using their structural MRI data. We first employed both VBM and ROI analyses to compare gray matter volume (GMV) and white matter volume (WMV) between 41 SZ patients and 42 age- and sex-matched NCs. The method of SVM combined with RFE was used to discriminate SZ patients from NCs using significant between-group differences in both GMV and WMV as input features. We found that SZ patients showed GM and WM abnormalities in several brain structures primarily involved in the emotion, memory, and visual systems. An SVM with a RFE classifier using the significant structural abnormalities identified by the VBM analysis as input features achieved the best performance (an accuracy of 88.4%, a sensitivity of 91.9%, and a specificity of 84.4%) in the discriminative analyses of SZ patients. These results suggested that distinct neuroanatomical profiles associated with SZ patients might provide a potential biomarker for disease diagnosis, and machine-learning methods can reveal neurobiological mechanisms in psychiatric diseases.

Abbreviations: ANOVA = analysis of variance, AUC = area under the curve, CAL = calcarine, CAU = caudate, CSF = cerebrospinal fluid, CUN = cuneus, FDR = false discovery rate, FFG = fusiform gyrus, FWHM = full-width at half-maximum, GLM = general linear model, GM = gray matter, GMV = gray matter volume, HIP = hippocampus, LING = lingual gyrus, MFG = middle frontal gyrus, MOG = middle occipital gyrus, MRI = magnetic resonance imaging, NCs = normal controls, PANSS = Positive and Negative Syndrome Scale, PCUN = precuneus, PHG = parahippocampal gyrus, PoCG = postcentral gyrus, RFE = recursive feature elimination, RGMV = regional gray matter volume, ROC = receiver operating characteristic, ROI = region of interest, RWMV = regional white matter volume, SCID = structured clinical interview according to the DSM-IV-TR, STG = superior temporal gyrus, SVM = support vector machine, SZ = schizophrenia, TBV = total brain volume, THM = thalamus, VBM = voxel-based morphometry, WM = white matter, WMV = white matter volume.

Keywords: recursive feature elimination, region of interest, schizophrenia, support vector machine, voxel-based morphometry

Editor: Bernhard Schaller.

XL and YY contributed equally to this study.

Funding: This study was supported by the National Natural Science Foundation of China (NSFC) (31400845, 81571333), Special Program for Applied Research on Super Computation of the NSFC-Guangdong Joint Fund (the second phase), the Guangdong Natural Science Foundation (S2012040007743, 2015A030313800), the Fundamental Research Funds of Central Universities under the South China University of Technology (2013ZM046, 2015ZZ042), the Medical Research Foundation of Guangdong (A2012523), the Science and Technology Program of Guangdong (2013B021800027), the Science and Technology Program of Guangzhou (2013J4100096, 2014Y2-00062, 201501010260), and the Guangzhou municipal key discipline in medicine for Guangzhou Brain Hospital (GBH2014-ZD04, GBH2014-QN06).

The authors have no conflicts of interest to disclose.

Supplemental Digital Content is available for this article.

[a] Department of Psychiatry, Guangzhou Brain Hospital (GBH)/(Guangzhou Huiai Hospital, The Affiliated Brain Hospital of Guangzhou Medical University), Guangzhou, China, [b] Department of Biomedical Engineering, School of Materials Science and Engineering, South China University of Technology (SCUT), Guangzhou, China, [c] GBH-SCUT Joint Research Centre for Neuroimaging, Guangzhou, China, [d] School of Medicine, South China University of Technology (SCUT), Guangzhou, China, [e] Department of Clinical Psychology, Guangzhou Brain Hospital (GBH)/ (Guangzhou Huiai Hospital, The Affiliated Brain Hospital of Guangzhou Medical University), Guangzhou, China, [f] Department of Radiology, Guangdong Academy of Medical Sciences, Guangdong General Hospital, Guangzhou, China, [g] School of Computer Science and Engineering, South China University of Technology (SCUT), Guangzhou, China, [h] Department of Biomedical Engineering, New Jersey Institute of Technology, NJ, US, [i] Department of Electric and Computer Engineering, New Jersey Institute of Technology, NJ, US, [j] Department of Psychiatry, Icahn School of Medicine at Mount Sinai, NY, US, [k] Department of Nuclear Medicine and Radiology, Institute of Development, Aging and Cancer, Tohoku University, Sendai, Japan, [l] Institute for Digital Communications, School of Engineering, The University of Edinburgh, Edinburgh EH9 3JL, UK.

[*] Correspondence: Department of Psychiatry, Guangzhou Brain Hospital (GBH)/(Guangzhou Huiai Hospital, The Affiliated Brain Hospital of Guangzhou Medical University), Guangzhou, China; Kai Wu, School of Material Science and Engineering Guangzhou, Guangdong, China (e-mail: kaiwu@scut.edu.cn)

Medicine (2016) 95:30(e3973)

Received: 20 January 2016 / Received in final form: 16 May 2016 / Accepted: 26 May 2016

http://dx.doi.org/10.1097/MD.0000000000003973

1. Introduction

Schizophrenia (SZ) is a disabling mental disorder characterized by delusions and auditory hallucinations, as well as impairments in memory, attention, executive, and many other high-order cognitive functions.[1,2] The development of magnetic resonance imaging (MRI) has offered an effective and noninvasive approach to examine the anatomy of the brain and has prompted numerous scientists to explore the underlying neuropathology of SZ. The vast majority of studies show that gray matter (GM) reductions in the brains of SZ patients typically involve the temporal, frontal, and parietal lobes.[3–7] GM abnormalities in the occipital lobe, insula, striatum, thalamus, cerebellum, and cingulate regions have also been reported.[8–12] White matter (WM) fibers link spatially distinct cortical and subcortical regions. Several studies have suggested that SZ is a type of disconnection syndrome [13,14]; thus, it is reasonable to hypothesize that WM aberrances are associated with this psychosis.[6,15] A number of studies have found white matter volume (WMV) reductions in the corpus callosum, bilateral frontal lobe, and internal capsule in SZ patients.[16–18]

However, these GM or WM deficits were identified using conventional univariate analyses at a group level, which can analyze group-wise differences in brain areas but generally cannot differentiate among the individuals in 2 or more groups. Recently, machine learning, which is a type of multivariate analysis that can automatically discriminate individuals within a sample group, was used to classify several neuropsychiatric disorders and addictions, such as SZ,[19–24] Alzheimer's disease,[25–28] depression,[29–31] attention-deficit hyperactivity disorder,[32–34] and smoking.[35]

Support vector machine (SVM) is a specific method of supervised machine learning that aims to classify data points by maximizing the margin between classes in a high-dimensional space.[36] Advantages of this method are the selection of training examples that are most informative for the classification and a good scaling for high dimensions. A previous study discriminated SZ patients from normal controls (NCs) by analyzing multimodal brain imaging data (EEG, structural MRI, and functional MRI) with a SVM classifier and achieved a good classification performance with a 91% accuracy and 100% prediction rate.[37] A more recent study applied the SVM method to the automatic classification of 72 SZ patients and 74 NCs and achieved an average accuracy of 80%.[38] These previous findings demonstrate the promising classification performance of the SVM method, as well as the potential for applying this method to identify biomarkers for the diagnosis of psychiatric diseases.

Recent studies have shown that feature reduction can increase computational speed and improve classification performance, by removing uninformative, irrelevant, or redundant features from the classification procedures.[27,39] A recursive feature elimination (RFE) algorithm is an iterative procedure that eliminates 1 backward feature at a time,[40] and thus, can prevent information loss that can occur by eliminating several features in 1 iteration.[41] Previous studies have indicated that RFE employed for dimensionality reduction can significantly improve classification accuracy of neuroimaging data [35] and yield a better classification performance than many other feature reduction methods.[40]

In this study, we employed voxel-based morphometry (VBM) and region of interest (ROI) analyses to compare differences in gray matter volume (GMV) and WMV between SZ patients and NCs. Significant between-group differences in GMV and WMV were selected as features in the discriminate analysis of 2 groups using SVM combined with RFE.

2. Materials and methods

2.1. Subjects

Forty-one SZ patients (the SZ group) and 42 age- and sex-matched NCs (the NC group) were included in this study. The SZ patients were diagnosed by trained and experienced clinical psychiatrists using a structured clinical interview according to the DSM-IV-TR (SCID).[42] The SZ and NC groups were recruited from Guangzhou Brain Hospital and the local community, respectively. All subjects were aged between 18 and 45 years, and their biological parents were Han Chinese. Before scanning, a clinical assessment was performed by psychiatrists using the Positive and Negative Syndrome Scale (PANSS).[43] The subjects obtained a consensus score for each item on all 3 subscales (positive symptoms, negative symptoms, and general psychopathology) that was based on a 7-point scale indicating the severity of the symptom (1 = absent; 2 = minimal; 3 = mild; 4 = moderate; 5 = moderate severe; 6 = severe; 7 = extreme).[44] The inclusion criteria for all SZ patients included the following: (1) a total score of at least 60 for the 3 PANSS subscales and (2) at least 3 positive symptom items on the PANSS with a score of at least 4.

The exclusion criteria for all subjects included the following: (1) any other psychiatric Axis I disorder meeting DSM-IV criteria, including schizoaffective disorders, mental retardation, major depressive disorder, bipolar disorder, delirium, dementia, memory disorder, and other cognitive disorders; (2) mental disorder due to substance dependence, a serious unstable somatic disease, definite diabetes, thyroid diseases, hypertension or heart disease; (3) narrow angle glaucoma; (4) a history of epilepsy, except for febrile convulsions; (5) alcohol dependence meeting DSM-IV-TR criteria (excluding nicotine dependence); (6) receiving electroconvulsive therapy within the past 6 months; (7) a contraindication for MRI; (8) medical resource neuroleptic malignant syndrome or serious tardive dyskinesia; (9) a serious suicide attempt or an irritative state; (10) noncompliant drug administration or a lack of legal guardians; or (11) lactating, pregnant, or planning pregnancy. In addition, the NCs were excluded if they had a first- or second-degree relative with a psychiatric Axis I disorder according to the DSM-IV criteria. Before enrollment, all subjects or their legal guardians provided written informed consent. These studies were performed according to the Declaration of Helsinki and approved by the Ethics Committees of the Guangzhou Brain Hospital.

2.2. MRI data acquisition

Imaging data were acquired using Philips 3T MR systems (Philips, Best, The Netherlands) located at Guangzhou Brain Hospital. For each subject, an anatomical image was obtained using a sagittal 3-dimensional gradient-echo T1-weighted sequence (TR = 7.6 ms, TED = 3.7 ms, TI = 795 ms, flip angle = 8°, 180 slices, slice thickness = 1 mm, Gap = 0 mm, matrix = 256×256, inversion time = 0).

2.3. Image processing

Image processes were described in our previous studies.[29,30,45] Briefly, all T1-weighted MRI data processing was performed using the SPM8 software package (http://www.fil.ion.ucl.ac.uk/spm; Institute of Neurology, University College London, UK).

First, each T1-weighted MRI was segmented into 3 tissue maps, including GM, WM, and cerebrospinal fluid (CSF) by using the new segmentation algorithm from SPM8. Second, a customized, population-specific template was created from the segmented tissue maps by using the DARTEL template-creation tool.[46] Third, all GM and WM maps were warped to the custom template space, using its corresponding smooth, reversible deformation parameters. A modulation was applied by locally multiplying tissue values by the Jacobian determinants derived from the special normalization step.[47] Finally, all warped, modulated GM and WM images were smoothed with an 8-mm full-width at half-maximum (FWHM) Gaussian kernel.

2.4. VBM analysis

Smoothed modulated GM and WM images were analyzed with SPM8 utilizing a general linear model (GLM). Voxel-wise GMV differences between the SZ and NC groups were investigated using analysis of variance (ANOVA). The covariates included in the model were total brain volume (TBV = total GMV + total WMV), age, gender, and years of education. The resulting statistical map was corrected for multiple comparisons to a significance level of $P < 0.05$ by combining individual voxels ($P < 0.001$) and using a cluster size of 173 voxels. This correction was confined within a whole-brain mask and determined using Monte Carlo simulations (FWHM = 8 mm, iterations = 1000) using the AFNI AlphaSim program (http://afni.nih.gov/afni/docpdf/AlphaSim.pdf).

2.5. ROI analysis

Recently, many studies have suggested the use of higher-resolution parcellation, of up to 1000 smaller parcels, instead of using a coarse parcellation scheme of AAL atlas including 90 brain regions.[48–50] Therefore, we parcellated the entire cerebrum into 1024 ROIs with equal sizes using a high-resolution automated anatomical labeling (AAL) atlas,[51] which was defined from the standard AAL atlas including 90 cerebral regions.[52] We then calculated the regional GMV (RGMV) and regional WMV (RWMV) in each of the 1024 ROIs from the modulated GM and WM images, respectively. ANOVAs were performed to compare the RGMV and RWMV in 1024 ROIs between the SZ and NC groups. The covariates included in the model were TBV, age, gender, and years of education. The significance level was $P < 0.05$, corrected by false discovery rate (FDR) correction.

2.6. Correlation between the PANSS and the RGMV or RWMV

We calculated the RGMV or RWMV of brain areas showing significant between-group differences in both the VBM and ROI analyses. The partial correlations between the PANSS scores (including positive, negative, and total scores of PANSS) and the RGMV or RWMV of brain areas were calculated, controlling for the age, gender, years of education, and TBV. The volumes of extracted brain areas and the partial correlations were calculated in Matlab 2010b using in-house scripts.

2.7. SVM with RFE

In this study, a classification method of SVM with RFE was applied to discriminate SZ patients from NCs using the significant between-group differences in RGMV and RWMV identified by the VBM and ROI analyses. SVM is an effective classification method based on the structural risk minimization principle.[41] It implements the following idea: input vectors are nonlinearly mapped to a high-dimension feature space.[53] In the feature space, the machine searches for an optimal hyperplane, which maximizes the distance from the hyperplane to the closest examples in each class to classify different groups. Once the hyperplane is found, it can be used to predict the group label of a new testing example. The symbols (+) and (–) are used to represent 2 classes. The input features and the class labels are given. A linear decision function is a simple weighted sum of the input vector plus a bias.[54] Given the nature of input features, a linear decision function was applied. The weight vector and bias value are represented by w and b, respectively. The decision function is:

$$D(x) = w.x + b$$

If $D(x)>0$, x belonged to class (+), else if $D(x)<0$, x belonged to class (–), else x was on the decision boundary. A linear kernel SVM implemented in the LIBSVM toolbox was used in this study.[55]

In machine learning, some features are uninformative, irrelevant, or redundant for classification, and too many features may cause "over-fitting.". Therefore, eliminating a number of features not only simplifies the classification model but also improves the classification accuracy.[56] The SVM-RFE algorithm uses the SVM classifier iteratively to remove redundant features while preserving discriminative features. RFE is an iterative procedure that trains the classifier and removes the smallest ranking criterion feature after ranking.[40] We chose the square of the feature weights w_i (w_i^2) of the decision function as the ranking criterion. Clearly, the smaller weight of a feature means the less contribution to the decision function. In each iteration, we computed the ranking criteria w_i^2 for all features and eliminated the feature corresponding to the smallest w_i^2. We obtained a discriminate feature list after n iterations.

The performance of the classifier is evaluated by leave-one-out cross-validation (LOOCV). The leave-one-out method is a cross-validation error estimation method.[57] The superiority of the leave-one-out method has been proven.[58,59] The LOOCV involves using data from all but 1 subject as a training set, and the remaining data are used as a test set. This process should be repeated until each sample is used to calculate the overall accuracy of SVM.

Furthermore, we plotted the receiver operating characteristic (ROC) curves and calculated the area under the curve (AUC) to examine the possibility of discriminating SZ patients and NCs correctly. The value of the AUC is between 0 and 1. It is generally believed that a value close to 1 indicates a better prediction performance. In addition to the accuracy and AUC, we measured the sensitivity and specificity to quantify the performance of the SVM. The definitions of sensitivity, specificity, and accuracy are as follows:

$$\text{Sensitivity} = \frac{\text{TP}}{\text{TP} + \text{FN}}$$

$$\text{Specificity} = \frac{\text{TN}}{\text{TN} + \text{FP}}$$

$$\text{Accuracy} = \frac{\text{TP} + \text{TN}}{\text{TN} + \text{FN} + \text{TN} + \text{TP}}$$

where TP is true positive, the number of positive subjects classified as positive; FN is false negative, the number of positive

Table 1

Demographic and clinical characteristics.

	SZ patients (n = 41)	NC (n = 42)	*t* value (x^2)	*P*
Age, y	25.68 ± 6.61	26.02 ± 6.227	−0.259	0.796
Gender, F/M	17:24	15:27	0.289	0.591†
Education years, y	11.07 ± 3.26	11.62 ± 2.241	−0.891	0.376
TBV, mm^3	1184.72 ± 120.57	1192.21 ± 109.31	0.297	0.767
Positive PANSS score	24.98 ± 3.921	7.07 ± 0.342	29.482	<0.0001*
Negative PANSS score	23.29 ± 7.281	8.4 ± 1.726	12.888	<0.0001*
Total PANSS score	43.07 ± 7.333	16.86 ± 0.256	22.587	<0.0001*

Values are showed as the mean ± SD.

F = female, M = male, NCs = normal controls, PANSS = Positive and Negative Syndrome Scale, SZ = schizophrenia, TBV = total brain volume.

* Statistical significance was set at $P<0.05$.

† For the gender distribution among the 2 groups, *P* value was obtained using the x^2 test.

subjects classified as negative; TN is true negative, the number of negative subjects classified as negative; and FP is false positive, the number of negative subjects classified as positive.

A permutation test was applied to evaluate the statistical significance of the classification results.[60] The permutation test is a type of nonparametric test and can be used to test a null hypothesis.[61] In our analysis, we permuted the class labels of the training data for 1000 times randomly and performed all classification process with each set of permuted class labels. Based on probability distributions, it is possible to test the null hypothesis indicated by a small *P* value. The *P* value was computed as the proportion of accuracies that are no less than the accuracy obtained by the original data. The statistical significance was set at $P < 0.05$.

3. Results

3.1. Clinical and demographic characteristics

The clinical and demographic characteristics of all subjects are shown in Table 1. There was no significant difference in age, gender, years of education, and TBV between the SZ and NC groups ($P > 0.05$). However, the positive, negative, and total scores for the PANSS in the SZ group were significantly higher than those in the NC group ($P < 0.0001$).

3.2. VBM analysis of GMV and WMV

The VBM analysis indicated that the SZ group showed significant GMV reductions in the left hippocampus (HIP) (Fig. 1A) and the right middle occipital gyrus (MOG) (Fig. 1B), as well as significant GMV increases in the right posterior lobe of the cerebellum (Fig. 1C), left caudate (CAU) (Fig. 1D), and left thalamus (THM) (Fig. 1D) when compared with the NC group. The SZ group showed significant WMV reductions in the right lingual gyrus (LING) (Fig. 2A), right calcarine (CAL) (Fig. 2A), and right cuneus (CUN) (Fig. 2B), as well as significant WMV increases in the right precuneus (PCUN) (Fig. 2C) when compared with the NC group.

3.3. ROI analysis of GMV and WMV

The ROI analysis indicated that the SZ group showed significant GMV reductions in the left MOG (Fig. 3A), the parahippocampal gyrus (PHG) (Fig. 3B), right MOG (Fig. 3C), and right postcentral gyrus (PoCG) (Fig. 3D), as well as significant GMV increases in the right PCUN (Fig. 3E) when compared with the NC group. The SZ group showed significant WMV reductions in the right LING (Fig. 4A), bilateral CAL (Fig. 4A), bilateral CUN (Fig. 4A), and left superior temporal gyrus (STG) (Fig. 4B), as well as significant WMV increases in the left middle frontal gyrus (MFG) (Fig. 4C), right PCUN (Fig. 4D), and right fusiform gyrus (FFG) (Fig. 4E) when compared with the NC group.

3.4. Correlation between PANSS and RGMV or RWMV

We calculated the RGMV or RWMV of 17 brain areas (as shown in Figs. 1–4), which showed significant between-group differences in both the VBM and ROI analyses. The RGMV of the left PHG, as well as the RWMV of the right PCUN and left STG indicated significant positive correlations with positive PANSS scores, after controlling for age, sex, years of education, and TBV (Fig. 5).

3.5. Overall classifier performance

Automatic classifications were performed to distinguish SZ patients from NCs. First, we applied the significant between-group differences for both RGMV and RWMV in the VBM analysis as the input features for the classifier. The linear SVM without RFE classifier achieved an accuracy of 82.6% ($P < 0.05$), a sensitivity of 83.8%, and a specificity of 81.3%; the linear SVM with RFE classifier yielded a better classification performance with an accuracy of 88.4% ($P < 0.05$), a sensitivity of 91.9%, and a specificity of 84.4% for the same input. Second, we applied the significant between-group differences for both RGMV and RWMV by the ROI analysis as the input features for the classifier. The linear SVM without RFE classifier achieved an accuracy of 79.5% ($P < 0.05$), a sensitivity of 71.4%, and a specificity of 87.8%; the linear SVM with RFE classifier achieved a slightly better performance with an accuracy of 80.7% ($P < 0.05$), a sensitivity of 73.8%, and a specificity of 87.8%. ROC curves were computed taking each subject's discriminative score as a threshold and are presented in Fig. 6. The areas under the ROC curve for the 4 classifiers were 0.915, 0.948, 0.895, and 0.887 (Table 2).

4. Discussion

In the present study, we applied a machine learning method that combined SVM with RFE to discriminate SZ patients from NCs using structural MRI data. Our results indicated that the SZ patients showed significant GM and WM abnormalities

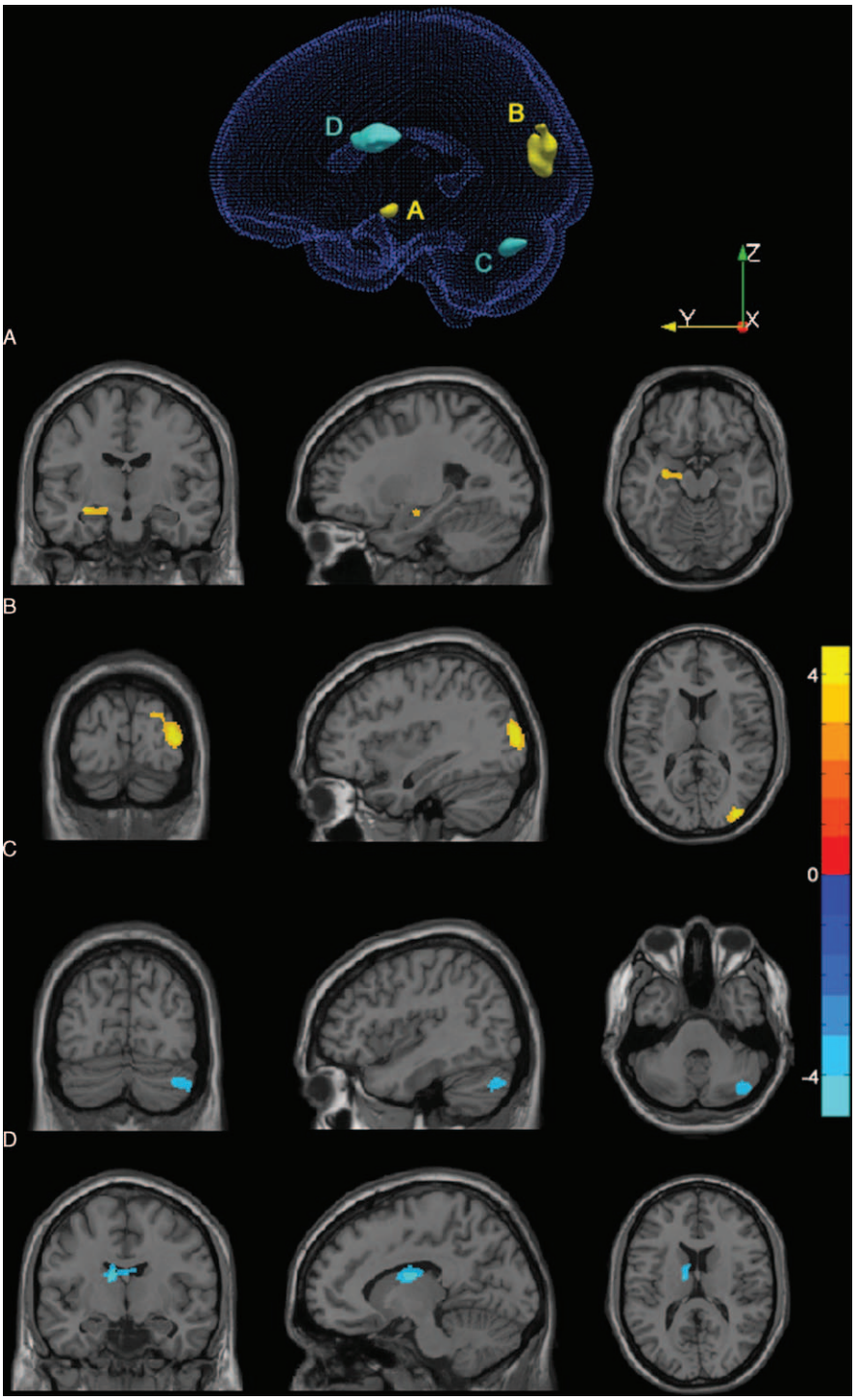

Figure 1. Gray matter volume abnormalities in schizophrenia patients compared with normal controls by the VBM analysis. Schizophrenia patients showed significant gray matter volume reductions (A and B) and increases (C and D). VBM = voxel-based morphometry.

primarily in the emotion, memory, and visual systems according to both the VBM and ROI analyses. In the discriminative analyses of SZ patients, the SVM with RFE classifier used with the significant structural abnormalities identified by the VBM analysis as input features achieved the best performances (an accuracy of 88.4%, a sensitivity of 91.9%, and a specificity of 84.4%), which was better than the performances of previous discriminative analyses of SZ patients using structural MRI data.[23,24]

In this study, we achieved better performances in the discriminative analyses of SZ patients using the SVM with RFE classifier, when compared with those using the SVM without RFE classifier. The machine learning method of SVM has been used to obtain available biomarkers in the diagnoses of psychiatric diseases and addictions.[23,62–64] However, some input features are irrelevant or redundant for classification when performing classification with SVM. Thus, the exclusion of uninformative features from the dataset while retaining

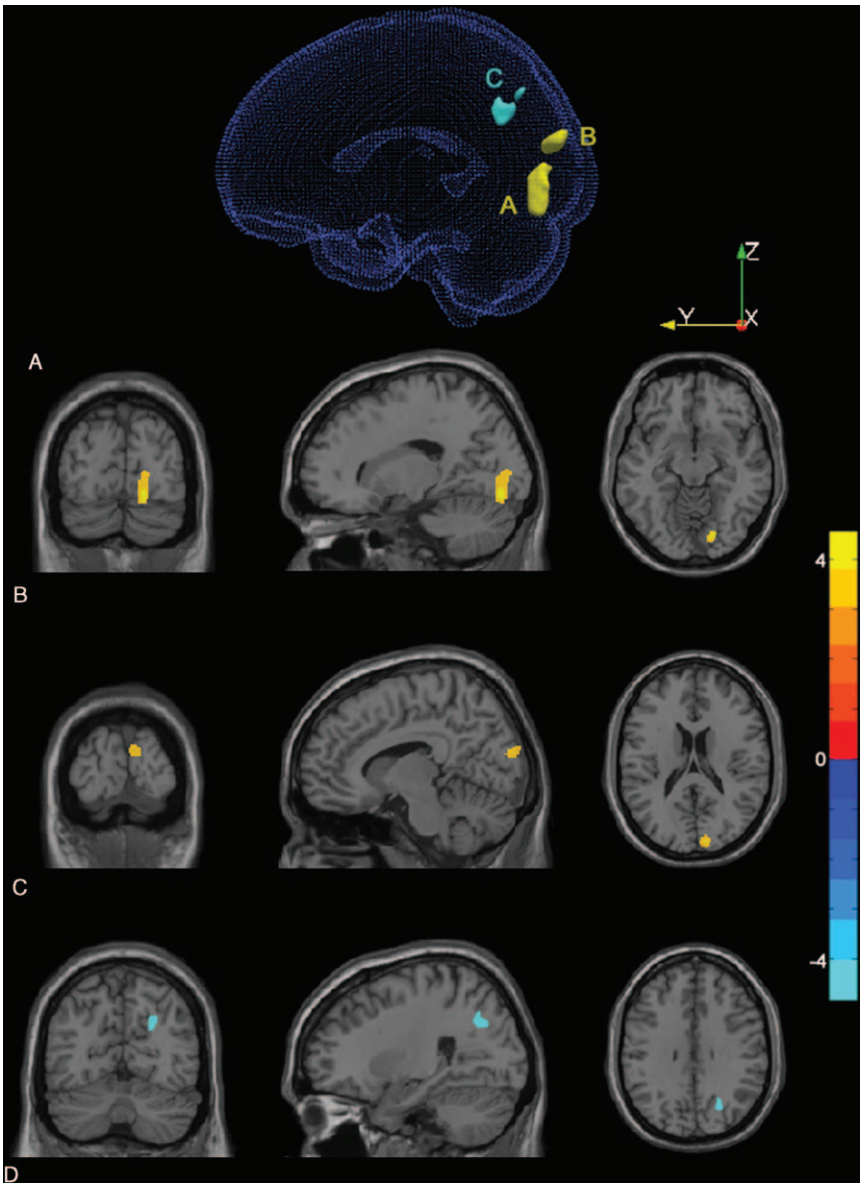

Figure 2. White matter volume abnormalities in schizophrenia patients compared with normal controls by the VBM analysis. Schizophrenia patients showed significant white matter volume reductions (A and B) and increases (C). VBM = voxel-based morphometry.

discriminative features can not only increase the computation speed but also improve the classification performance.[65,66] A previous study by our group selected features based on their rankings of discriminative power by computing F-scores individually and independently and achieved a good result in the discriminative analysis of depressive patients with structural MRI data.[29] A more recent study applied VBM with a multivariate classification method consisting of a SVM with RFE to discriminate smokers from nonsmokers using their structural MRI data and achieved the highest accuracy of 69.6%.[35]

In addition to using dimensionality reduction, the feature characters (i.e., structural and functional characteristics) and spatial resolution of brain areas might also affect the classification accuracy. A previous study introduced an M3 method to identify AD patients by combining multimodal imaging and multilevel measures and demonstrated promising classification performance (a classification accuracy of 89.47%, a sensitivity of 87.50%, and a specificity of 90.91%).[26] In this study, we compared both GM and WM structures between SZ patients and NCs and then applied these structural abnormalities as input features of discriminate analyses. Our results verified that multiple structural characteristics were useful in increasing the classification performance (see supplementary Table S1, http://links.lww.com/MD/B107). Moreover, in the previous study,[35] the SVM-RFE procedure was applied separately on raw GMVs, mean GMVs from the standard AAL atlas (including 90 cerebral areas) and from the high resolution AAL atlas (including 1024 cerebral areas), and it achieved the highest accuracy when the high-resolution AAL atlas was used. However, our results were inconsistent with this finding and indicated that the classifiers using the input features from the VBM analysis achieved better performances than those using the input features from the ROI analysis. The reason for this inconsistency might be the significant

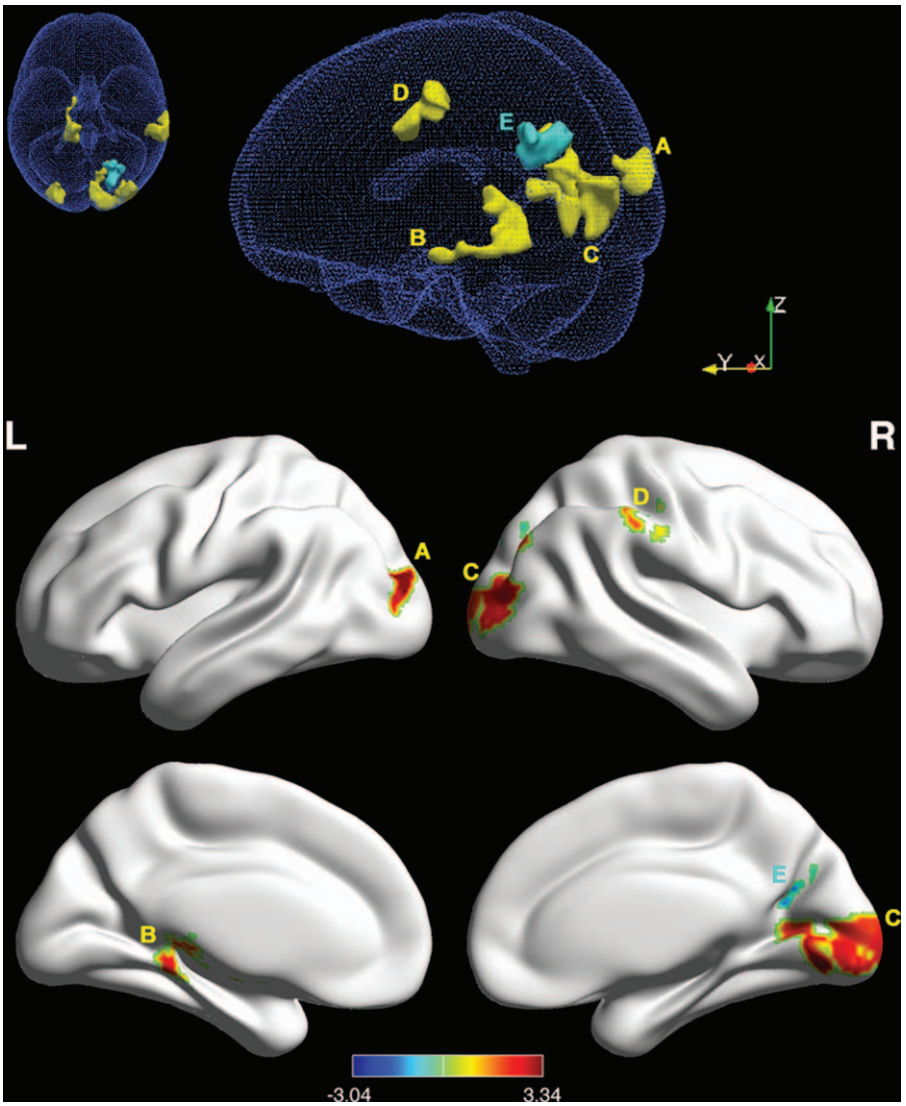

Figure 3. Gray matter volume abnormalities in schizophrenia patients compared with normal controls by the ROI analysis. Schizophrenia patients showed significant gray matter volume reductions (A–D) and increases (E). ROI = region of interest.

between-groups differences of GMVs in the VBM analysis but not raw GMVs that were adopted as the input features of classifiers in this study.

In this study, we found significant GM and WM abnormalities in many brain areas involved primarily in the emotion, memory, and visual systems, which were consistent with many previous studies.[67–75] More importantly, several important brain areas related to emotion processing and memory functions, such as the left PHG, left STG, and right PCUN, showed significant positive correlations between their RGMV or RWMV and positive PANSS scores. These results were largely consistent with a previous multimodal MRI studies that indicated that SZ patients showed lower values of canonical variants in subcortical regions, including the thalamus, striatum, hippocampus, parahippocampal gyrus, and visual cortex.[76]

It has been reported that SZ patients show emotional processing deficits in identifying emotions, understanding the feelings of others, inferring people's thoughts, and responding emotionally to others.[77] Our results indicated that SZ patients showed increased RGMV in the left CAU and left THM, which is consistent with previous findings in chronic SZ patients.[78,79] Interestingly, the increased RGMV in the CAU are thought to be related to antipsychotic usage.[80] The striatum is an essential neural system in emotional learning that receives sensory input and identifying stimuli that predict rewarding or reinforcing outcomes.[81,82] Moreover, our results indicated that SZ patients showed reduced RWMV in the left STG, which plays an important role in the recognition of learned social-emotional values, especially nonverbal social cues,[81] and is one of the most consistent regions showing significant structural abnormalities in SZ patients.[3,83] A recent functional near-infrared spectroscopy study showed that the fronto-temporal dysfunction is involved in the pathophysiology of abnormal emotional processing and cognitive inhibition in SZ patients.[84] We also found significant increases in RGMV and RWMV in the right PCUN, which is linked to self-awareness, mentalizing, and the theory of mind.[85,86] Reduced structural and functional connectivity among the amygdala, PCUN, and parietal regions might contribute to abnormalities in emotional processing in SZ patients.[87,88]

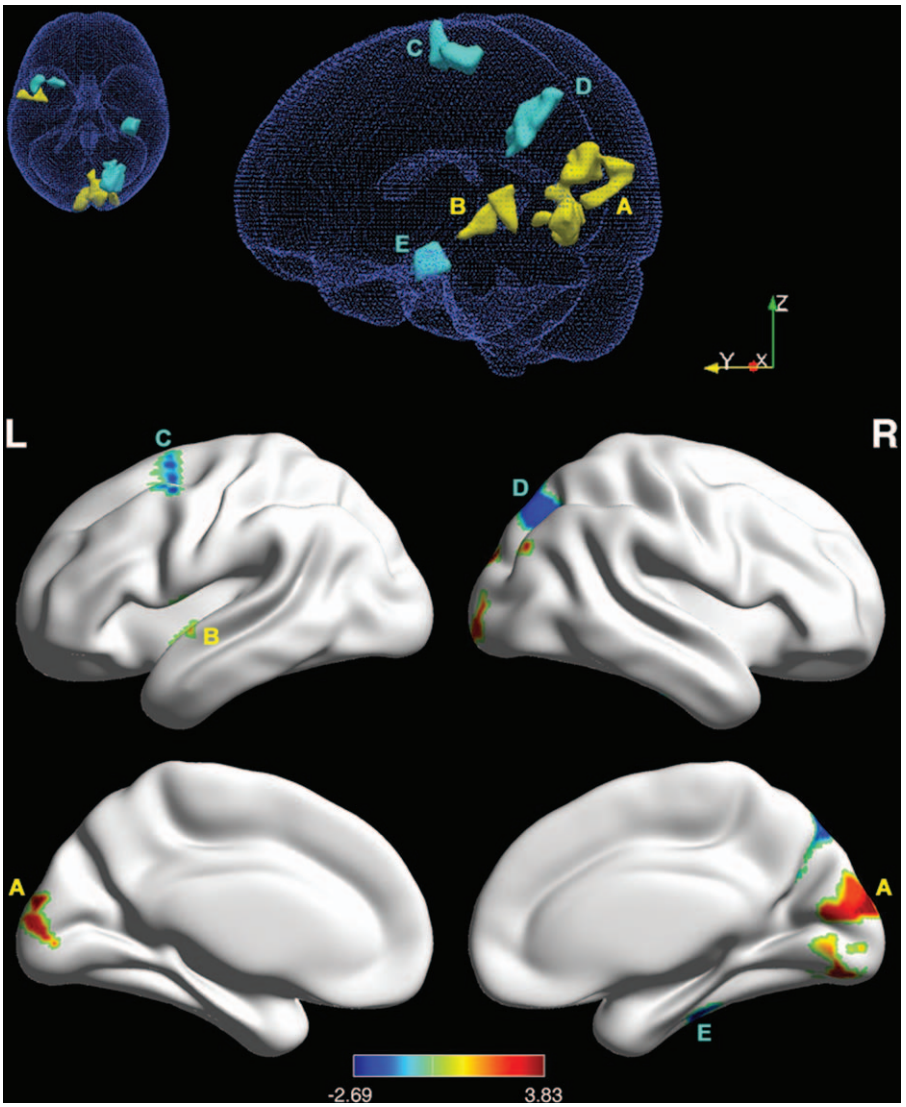

Figure 4. White matter volume abnormalities in schizophrenia patients compared with normal controls by the ROI analysis. Schizophrenia patients showed significant white matter volume reductions (A and B) and increases (C–E). ROI = region of interest.

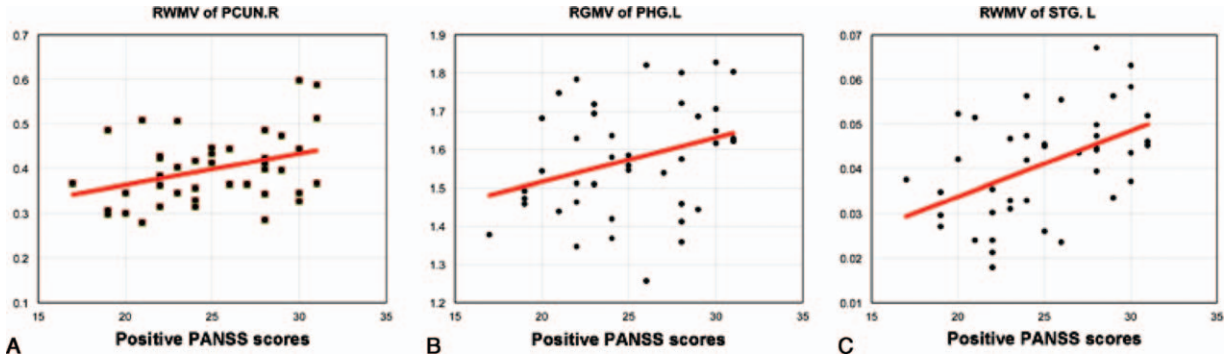

Figure 5. Significant positive correlations between the RGMV or RWMV of ROIs and positive PANSS scores, controlling for age, sex, education years, and TBV: (A) RWMV of PCUN.R; (B) RGMV of PHG.L; (C) RWMV of STG.L. ROI = region of interest, RGMV = regional gray matter volume, RWMV = regional white matter volume, PCUN.R = right precuneus, PHG.L = left parahippocampal gyrus, STG.L = left superior temporal gyrus, PANSS = positive and negative syndrome scale, TBV = total brain volume.

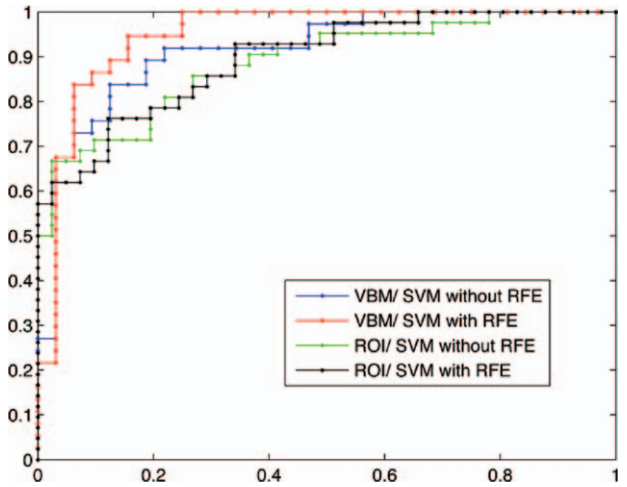

Figure 6. ROC curves of automatic classifications. Significant between-group differences of both RGMV and RWMV by the VBM analysis were used as the input features of the linear SVM without RFE (blue line) and with RFE (red line). Significant between-group differences of both RGMV and RWMV by the ROI analysis were used as the input features of the linear SVM without RFE (green line) and with RFE (black line). RFE = recursive feature elimination, ROC = receiver operating characteristic, ROI = region of interest, RGMV = regional gray matter volume, RWMV = regional white matter volume, SVM = support vector machine, VBM = voxel-based morphometry.

Table 2

Classification performances.

	Sensitivity	Specificity	Accuracy	AUC
VBM/SVM without RFE	83.8%	81.3%	82.6%	0.915
VBM/SVM with RFE	91.9%	84.4%	88.4%	0.948
ROI/SVM without RFE	71.4%	87.8%	79.5%	0.887
ROI/SVM with RFE	73.8%	87.8%	80.7%	0.895

AUC = area under the curve, RFE = recursive feature elimination, ROI = region of interest, SVM = support vector machine, VBM = voxel-based morphometry.

Pronounced deficits in memory, including episodic memory and semantic memory, are also affected in the daily life of SZ patients.[89,90] Our results indicated that the SZ patients showed reduced RGMV in the left HIP and left PHG, which is consistent with previous studies.[6,91] The HIP contributes to the recollection of contextual information in the service of relative memory tasks and is one of the most prominent impaired brain regions in both first-episode and chronic SZ patients.[91,92] In addition, a previous study demonstrated reduced functional and anatomical connectivity between HIP and some brain areas, such as the posterior cingulate cortex, medial prefrontal cortex, and PHG.[93] Reduced hippocampal volume and aberrant hippocampal modulation might work together to impair episodic memory in SZ patients.

SZ patients have impairments in higher-order processing and primary functions, such as visual processing.[94] In this study, we found significant GM and WM abnormalities in the visual cortex, including the bilateral MOG, bilateral CAL, bilateral CUN, right FFG, and right LING. GM and WM abnormalities in the primary visual areas and visual association areas of SZ patients have been well documented.[95–97] As for the clinical symptoms, SZ patients sometimes experience visual hallucinations, which is associated with activity in the visual association areas.[98] A previous ROI study revealed a significant GMV reduction in the bilateral visual association areas in chronic SZ patients.[96] More recently, a study showed that SZ patients had a lower magnetization transfer ratio and fractional anisotropy in WM adjacent to visual areas.[97] Thus, our findings may support the notion that both dysfunction of visual areas and disconnections between them and other brain areas contribute to the impaired visual processing in SZ patients.

There are several limitations to this study. First, the sample size was modest. The VBM and ROI analyses with relatively small sample sizes in this study might have insufficient statistical power and were at risk for false-positive errors. Moreover, a large number of subjects can train a more robust model to discriminate SZ patients from NCs. Second, the SZ patients included in this study were chronic SZ patients, and their brain structures might be affected by antipsychotic use. We plan to recruit first-episode, treatment-naive SZ patients in future studies. Third, although we analyzed both GM and WM structures and applied the abnormalities found in SZ patients into the machine learning study, multimodal MRI data including structural and functional MRI data will be useful for achieving better performance in a discriminative analysis. Fourth, this study suffered from that neuropsychological tests were not performed. In the future study, we plan to collect the data of the Measurement and Treatment Research to Improve Cognition in Schizophrenia (MATRICS) Consensus Cognitive Battery (MCCB), which provides a reliable and valid assessment of cognition across major cognitive domains.

5. Conclusion

In this study, we demonstrated that SZ patients showed GM and WM abnormalities in a variety of brain structures but primarily in the memory, visual, and emotion systems. The SVM-RFE classification showed good performance in distinguishing SZ patients from NCs by using structural features from structural MRI data. Distinct neuroanatomical profiles associated with SZ patients can provide a potential biomarker for disease diagnosis.

References

[1] Wheeler AL, Voineskos AN. A review of structural neuroimaging in schizophrenia: from connectivity to connectomics. Front Hum Neurosci 2014;8:653.
[2] van Os J, Kenis G, Rutten BP. The environment and schizophrenia. Nature 2010;468:203–12.
[3] Gupta CN, Calhoun VD, Rachakonda S, et al. Patterns of gray matter abnormalities in schizophrenia based on an international mega-analysis. Schizophr Bull 2015;41:1133–42.
[4] van den Heuvel MP, Fornito A. Brain networks in schizophrenia. Neuropsychol Rev 2014;24:32–48.
[5] Vita A, et al. Progressive loss of cortical gray matter in schizophrenia: a meta-analysis and meta-regression of longitudinal MRI studies. Transl Psychiatry 2012;2:e190.
[6] Sui J, Pearlson GD, Du Y, et al. In search of multimodal neuroimaging biomarkers of cognitive deficits in schizophrenia. Biol Psychiatry 2015;78:794–804.
[7] Li X, et al. Structural abnormalities in language circuits in genetic high-risk subjects and schizophrenia patients. Psychiatry Res 2012;201:182–9.
[8] Tohid H, Faizan M, Faizan U. Alterations of the occipital lobe in schizophrenia. Neurosciences (Riyadh) 2015;20:213–24.
[9] Meisenzahl EM, Koutsouleris N, Bottlender R, et al. Structural brain alterations at different stages of schizophrenia: A voxel-based morphometric study. Schizophrenia Res 2008;104:44–60.
[10] Lui S, Deng W, Huang XQ, et al. Neuroanatomical differences between familial and sporadic schizophrenia and their parents: An optimized voxel-based morphometry study. Psychiatry Res Neuroimaging 2009;171:71–81.

[11] Xu L, et al. Source-based morphometry: the use of independent component analysis to identify gray matter differences with application to schizophrenia. Human Brain Mapping 2009;30:711–24.
[12] Byne W, Hazlett EA, Buchsbaum MS, et al. The thalamus and schizophrenia: current status of research. Acta Neuropathol 2009; 117:347–68.
[13] Friston KJ. Disconnection and cognitive dysmetria in schizophrenia. Am J Psychiatry 2005;162:429–32.
[14] Stephan KE, Baldeweg T, Friston KJ. Synaptic plasticity and dysconnection in schizophrenia. Biol Psychiatry 2006;59:929–39.
[15] Ellison-Wright I, Bullmore E. Meta-analysis of diffusion tensor imaging studies in schizophrenia. Schizophr Res 2009;108:3–10.
[16] Lei W, et al. White matter alterations in first episode treatment-naive patients with deficit schizophrenia: a combined VBM and DTI study. Sci Rep 2015;5:12994.
[17] Watson DR, et al. A voxel based morphometry study investigating brain structural changes in first episode psychosis. Behav. Brain Res 2012; 227:91–9.
[18] Di X, Chan RCK, Gong QY. White matter reduction in patients with schizophrenia as revealed by voxel-based morphometry: an activation likelihood estimation meta-analysis. Prog Neuropsychopharmacol Biol Psychiatry 2009;33:1390–4.
[19] Su L, Wang L, Shen H, et al. Discriminative analysis of non-linear brain connectivity in schizophrenia: an fMRI Study. Front Hum Neurosci 2013;7:702.
[20] Shen H, Wang L, Liu Y, et al. Discriminative analysis of resting-state functional connectivity patterns of schizophrenia using low dimensional embedding of fMRI. Neuroimage 2010;49:3110–21.
[21] Kasparek T, Thomaz CE, Sato JR, et al. Maximum-uncertainty linear discrimination analysis of first-episode schizophrenia subjects. Psychiatry Res 2011;191:174–81.
[22] Tanaka S, Maezawa Y, Kirino E. Classification of schizophrenia patients and healthy controls using p100 event-related potentials for visual processing. Neuropsychobiology 2013;68:71–8.
[23] Nieuwenhuis M, van Haren NE, Hulshoff Pol HE, et al. Classification of schizophrenia patients and healthy controls from structural MRI scans in two large independent samples. Neuroimage 2012;61:606–12.
[24] Greenstein D, Malley JD, Weisinger B, et al. Using multivariate machine learning methods and structural MRI to classify childhood onset schizophrenia and healthy controls. Front Psychiatry 2012;3:53.
[25] Kloppel S, Stonnington CM, Chu C, et al. Automatic classification of MR scans in Alzheimers disease. Brain 2008;131:681–9.
[26] Dai Z, Yan C, Wang Z, et al. Discriminative analysis of early Alzheimer's disease using multi-modal imaging and multi-level characterization with multi-classifier (M3). Neuroimage 2012;59:2187–95.
[27] Zhou L, Wang L, Liu L, et al. Discriminative brain effective connectivity analysis for Alzheimer's disease: a kernel learning approach upon sparse Gaussian Bayesian network. Conf Comput Vis Pattern Recognit Workshops 2013;2013:2243–50.
[28] Li S, Shi F, Pu F, et al. Hippocampal shape analysis of Alzheimer disease based on machine learning methods. Am J Neuroradiol 2007;28: 1339–45.
[29] Chi M, Guo S, Ning Y, et al. Discriminative analysis of major depressive disorder and anxious depression using support vector machine. J Comput Theor Nanosci 2015;12:1395–401.
[30] Chi MY, Guo SW, Ning YP, et al. Using support vector machine to identify imaging biomarkers of major depressive disorder and anxious depression. Bio-Inspired Computing—Theories and Applications. Vol 472 2014;Berlin:Springer, 63–67.
[31] Gong Q, Wu Q, Scarpazza C, et al. Prognostic prediction of therapeutic response in depression using high-field MR imaging. Neuroimage 2011;55:1497–503.
[32] Iannaccone R, Hauser TU, Ball J, et al. Classifying adolescent attention-deficit/hyperactivity disorder (ADHD) based on functional and structural imaging. Eur Child Adolesc Psychiatry 2015;24:1279–89.
[33] Zhu CZ, Zang YF, Liang M, et al. Discriminative analysis of brain function at resting-state for attention-deficit/hyperactivity disorder. Medical Image Computing and Computer-Assisted Intervention: MICCAI International Conference on Medical Image Computing and Computer-Assisted Intervention. Vol 8 2005;Berlin:Springer, 468–475.
[34] Zhu C-Z, Zang Y-F, Cao Q-J, et al. Fisher discriminative analysis of resting-state brain function for attention-deficit/hyperactivity disorder. NeuroImage 2008;40:110–20.
[35] Ding X, Yang Y, Stein EA, et al. Multivariate classification of smokers and nonsmokers using SVM-RFE on structural MRI images. Human Brain mapping 2015;36:4869–79.
[36] Cherkassky V. The nature of statistical learning theory. IEEE Trans Neural Netw 1997;8:1564.
[37] Sui J, Castro E, He H, et al. Combination of FMRI-SMRI-EEG data improves discrimination of schizophrenia patients by ensemble feature selection. Conf Proc IEEE Eng Med Biol Soc 2014;2014:3889–92.
[38] Savio A, Graña M. Local activity features for computer aided diagnosis of schizophrenia on resting-state fMRI. Neurocomputing 2015;164: 154–61.
[39] Liang Y, Zhang F, Wang J, et al. Prediction of drought-resistant genes in Arabidopsis thaliana using SVM-RFE. PLoS One 2011;6:e21750.
[40] Guyon I, Weston J, Barnhill S. Gene selection for cancer classification using support vector machines. Mach Learn 2002;46:389–422.
[41] Yoon S, Kim S. Mutual information-based SVM-RFE for diagnostic classification of digitized mammograms. Pattern Recognit Lett 2009; 30:1489–95.
[42] First MB. User's Guide for the Structured Clinical Interview for DSM-IV Axis II Personality Disorders: SCID-II. 1997;Washington, DC:American Psychiatric Press, 91.
[43] Kay SR, Fiszbein A, Opler LA. The positive and negative syndrome scale (PANSS) for schizophrenia. Schizophr Bull 1987;13:261–76.
[44] van Tol MJ, van der Meer L, Bruggeman R, et al. Voxel-based gray and white matter morphometry correlates of hallucinations in schizophrenia: The superior temporal gyrus does not stand alone. Neuroimage Clin 2014;4:249–57.
[45] Qi H, Ning Y, Li J, et al. Gray matter volume abnormalities in depressive patients with and without anxiety disorders. Medicine 2014;93:e345.
[46] Ashburner J. A fast diffeomorphic image registration algorithm. Neuroimage 2007;38:95–113.
[47] Good CD, Johnsrude I, Ashburner J, et al. Cerebral asymmetry and the effects of sex and handedness on brain structure: a voxel-based morphometric analysis of 465 normal adult human brains. Neuroimage 2001;14:685–700.
[48] Bai F, Shu N, Yuan Y, et al. Topologically convergent and divergent structural connectivity patterns between patients with remitted geriatric depression and amnestic mild cognitive impairment. J Neurosci 2012; 32:4307–18.
[49] Cao M, Wang JH, Dai ZJ, et al. Topological organization of the human brain functional connectome across the lifespan. Dev Cogn Neurosci 2014;7:76–93.
[50] Wang J, Zuo X, Dai Z, et al. Disrupted functional brain connectome in individuals at risk for Alzheimer's disease. Biol Psychiatry 2013;73: 472–81.
[51] Zalesky A, Fornito A, Harding IH, et al. Whole-brain anatomical networks: does the choice of nodes matter? Neuroimage 2010;50: 970–83.
[52] Tzourio-Mazoyer N, Landeau B, Papathanassiou D, et al. Automated anatomical labeling of activations in SPM using a macroscopic anatomical parcellation of the MNI MRI single-subject brain. Neuroimage 2002;15:273–89.
[53] Cortes C, Vapnik V. Support-vector networks. Mach Learn 1995;20: 273–97.
[54] Duda RO, Hart PE. Pattern Classification and Scene Aanalysis. 1973; New York:Wiley, 482.
[55] Chang CC, Lin CJ. LIBSVM: a library for support vector machines. ACM Trans Intell Syst Technol 2011;2: Article 27.
[56] Ding J, Shi J, Wu FX. SVM-RFE based feature selection for tandem mass spectrum quality assessment. Int J Data Min Bioinform 2011;5: 73–88.
[57] Kim DR, Ali M, Sur D, et al. Determining optimal neighborhood size for ecological studies using leave-one-out cross validation. Int J Health Geogr 2012;11:10.
[58] Elisseeff A, Pontil M. Leave one out error and stability of learning algorithms with applications. Advances in Learning Theory: Methods, Models and Application—NATO Science Series III: Computer and Systems Science 2003;1–15.
[59] Kearns M, Ron D. Algorithmic stability and sanity-check bounds for leave-one-out cross-validation. Neural Comput 1999;11:1427–53.
[60] Golland P, Fischl B. Permutation tests for classification: towards statistical significance in image-based studies. Inf Process Med Imaging 2003;18:330–41.
[61] Liu F, Guo W, Fouche JP, et al. Multivariate classification of social anxiety disorder using whole brain functional connectivity. Brain Struct Funct 2015;220:101–15.
[62] Ding X, Yang Y, Stein EA, et al. Multivariate classification of smokers and nonsmokers using SVM-RFE on structural MRI images. Hum Brain Mapp 2015;36:4869–79.

[63] Fan Y, et al. Unaffected family members and schizophrenia patients share brain structure patterns: A high-dimensional pattern classification study. Biol Psychiatry 2008;63:118–24.
[64] Caprihan A, Pearlson GD, Calhoun VD. Application of principal component analysis to distinguish patients with schizophrenia from healthy controls based on fractional anisotropy measurements. Neuroimage 2008;42:675–82.
[65] Pereira F, Mitchell T, Botvinick M. Machine learning classifiers and fMRI: a tutorial overview. Neuroimage 2009;45((1 Suppl)):S199–209.
[66] Dosenbach NU, Nardos B, Cohen AL, et al. Prediction of individual brain maturity using fMRI. Science 2010;329:1358–61.
[67] Guo W, Hu M, Fan X, et al. Decreased gray matter volume in the left middle temporal gyrus as a candidate biomarker for schizophrenia: a study of drug naive, first-episode schizophrenia patients and unaffected siblings. Schizophr Res 2014;159:43–50.
[68] Lyu H, Hu M, Eyler LT, et al. Regional white matter abnormalities in drug-naive, first-episode schizophrenia patients and their healthy unaffected siblings. Aust N Z J Psychiatry 2015;49:246–54.
[69] Hu M, Li J, Eyler L, et al. Decreased left middle temporal gyrus volume in antipsychotic drug-naive, first-episode schizophrenia patients and their healthy unaffected siblings. Schizophr Res 2013;144:37–42.
[70] Goghari VM, Rehm K, Carter CS, et al. Regionally specific cortical thinning and gray matter abnormalities in the healthy relatives of schizophrenia patients. Cereb Cortex 2007;17:415–24.
[71] Fornito A, Yucel M, Patti J, et al. Mapping grey matter reductions in schizophrenia: an anatomical likelihood estimation analysis of voxel-based morphometry studies. Schizophr Res 2009;108:104–13.
[72] Bora E, Fornito A, Radua J, et al. Neuroanatomical abnormalities in schizophrenia: a multimodal voxelwise meta-analysis and meta-regression analysis. Schizophr Res 2011;127:46–57.
[73] Rajarethinam R, Sahni S, Rosenberg DR, et al. Reduced superior temporal gyrus volume in young offspring of patients with schizophrenia. Am J Psychiatry 2004;161:1121–4.
[74] Kuroki N, Shenton ME, Salisbury DF, et al. Middle and inferior temporal gyrus gray matter volume abnormalities in first-episode schizophrenia: an MRI study. Am J Psychiatry 2006;163:2103–10.
[75] Onitsuka T, Shenton ME, Salisbury DF, et al. Middle and inferior temporal gyrus gray matter volume abnormalities in chronic schizophrenia: an MRI study. Am J Psychiatry 2004;161:1603–11.
[76] Sui J, Pearlson GD, Du Y, et al. In search of multimodal neuroimaging biomarkers of cognitive deficits in schizophrenia. Biol Psychiatry 2015;78:794–804.
[77] Green MF, Horan WP, Lee J. Social cognition in schizophrenia. Nat Rev Neurosci 2015;16:620–31.
[78] Glahn DC, Laird AR, Ellison-Wright I, et al. Meta-analysis of gray matter anomalies in schizophrenia: application of anatomic likelihood estimation and network analysis. Biol Psychiatry 2008;64:774–81.
[79] Hulshoff Pol HE, Schnack HG, Mandl RC, et al. Focal gray matter density changes in schizophrenia. Arch Gen Psychiatry 2001;58:1118–25.
[80] Okugawa G, Nobuhara K, Takase K, et al. Olanzapine increases grey and white matter volumes in the caudate nucleus of patients with schizophrenia. Neuropsychobiology 2007;55:43–6.
[81] Ochsner KN. The social-emotional processing stream: five core constructs and their translational potential for schizophrenia and beyond. Biol Psychiatry 2008;64:48–61.
[82] Schultz W. Neural coding of basic reward terms of animal learning theory, game theory, microeconomics and behavioural ecology. Curr Opin Neurobiol 2004;14:139–47.
[83] Shenton ME, Dickey CC, Frumin M, et al. A review of MRI findings in schizophrenia. Schizophrenia Res 2001;49:1–52.
[84] Egashira K, Matsuo K, Nakashima M, et al. Blunted brain activation in patients with schizophrenia in response to emotional cognitive inhibition: a functional near-infrared spectroscopy study. Schizophr Res 2015;162:196–204.
[85] Mar RA. The neural bases of social cognition and story comprehension. Annu Rev Psychol 2011;62:103–34.
[86] Van Overwalle F, Baetens K. Understanding others' actions and goals by mirror and mentalizing systems: a meta-analysis. Neuroimage 2009;48:564–84.
[87] Mukherjee P, Whalley HC, McKirdy JW, et al. Lower effective connectivity between amygdala and parietal regions in response to fearful faces in schizophrenia. Schizophrenia Res 2012;134:118–24.
[88] Nazeri A, Chakravarty MM, Felsky D, et al. Alterations of superficial white matter in schizophrenia and relationship to cognitive performance. Neuropsychopharmacology 2013;38:1954–62.
[89] Aleman A, Hijman R, de Haan EHF, et al. Memory impairment in schizophrenia: a meta-analysis. Am J Psychiatry 1999;156:1358–66.
[90] Pender NP. From conditioning to conscious recollection: memory systems of the brain. Trends Cognitive Sci 2002;6:224–5.
[91] Adriano F, Caltagirone C, Spalletta G. Hippocampal volume reduction in first-episode and chronic schizophrenia: a review and meta-analysis. Neuroscientist 2012;18:180–200.
[92] Ranganath C, Minzenberg MJ, Ragland JD. The cognitive neuroscience of memory function and dysfunction in schizophrenia. Biol Psychiatry 2008;64:18–25.
[93] Zhou Y, Shu N, Liu Y, et al. Altered resting-state functional connectivity and anatomical connectivity of hippocampus in schizophrenia. Schizophr Res 2008;100:120–32.
[94] Kim D, Zemon V, Saperstein A, et al. Dysfunction of early-stage visual processing in schizophrenia: harmonic analysis. Schizophr Res 2005;76:55–65.
[95] Ananth H, Popescu I, Critchley HD, et al. Cortical and subcortical gray matter abnormalities in schizophrenia determined through structural magnetic resonance imaging with optimized volumetric voxel-based morphometry. Am J Psychiatry 2002;159:1497–505.
[96] Onitsuka T, McCarley RW, Kuroki N, et al. Occipital lobe gray matter volume in male patients with chronic schizophrenia: a quantitative MRI study. Schizophrenia Res 2007;92:197–206.
[97] Palaniyappan L, Al-Radaideh A, Mougin O, et al. Combined white matter imaging suggests myelination defects in visual processing regions in schizophrenia. Neuropsychopharmacology 2013;38:1808–15.
[98] Silbersweig DA, Stern E, Frith C, et al. A functional neuroanatomy of hallucinations in schizophrenia. Nature 1995;378:176–9.